

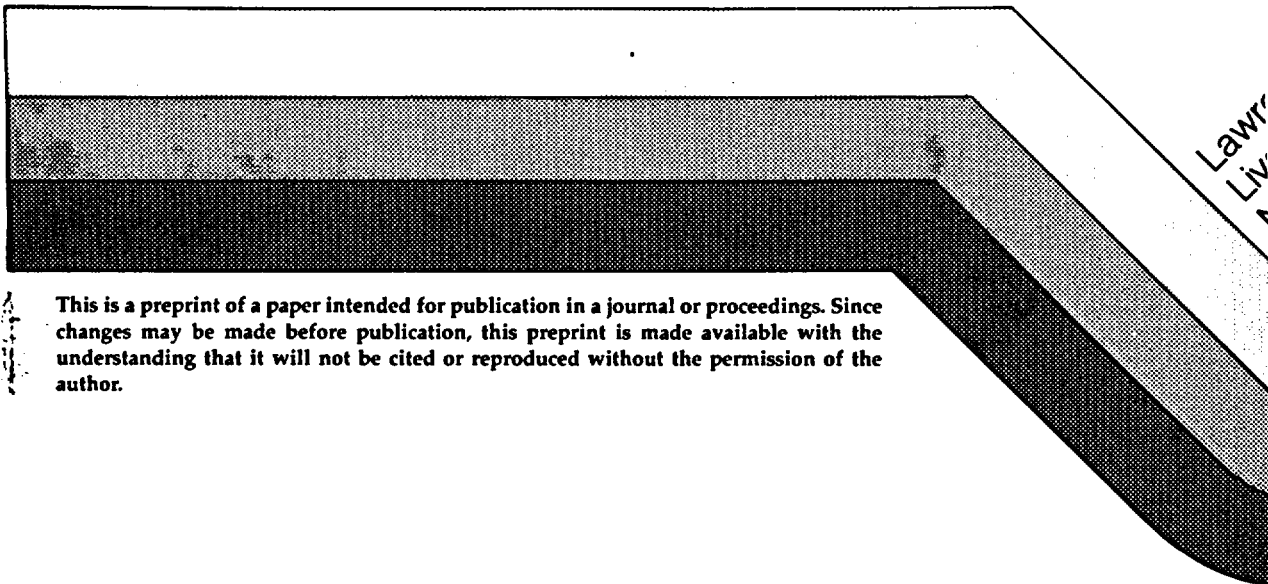
UCRL- 99734
PREPRINT

URANIUM TRANSPORT IN TOPOPAH SPRING TUFF:
AN ION-MICROSCOPE INVESTIGATION

K. D. McKeegan
D. Phinney
V. M. Oversby
M. Buchholtz-ten Brink
D. K. Smith

Submitted to
Materials Research Society Meeting
Berlin, Germany
October 1988

October 1988



This is a preprint of a paper intended for publication in a journal or proceedings. Since changes may be made before publication, this preprint is made available with the understanding that it will not be cited or reproduced without the permission of the author.

HYDROLOGY DOCUMENT NUMBER 624

DISCLAIMER

This document was prepared as an account of work sponsored by an agency of the United States Government. Neither the United States Government nor the University of California nor any of their employees, makes any warranty, express or implied, or assumes any legal liability or responsibility for the accuracy, completeness, or usefulness of any information, apparatus, product, or process disclosed, or represents that its use would not infringe privately owned rights. Reference herein to any specific commercial products, process, or service by trade name, trademark, manufacturer, or otherwise, does not necessarily constitute or imply its endorsement, recommendation, or favoring by the United States Government or the University of California. The views and opinions of authors expressed herein do not necessarily state or reflect those of the United States Government or the University of California, and shall not be used for advertising or product endorsement purposes.

Prepared by Yucca Mountain Project (YMP) participants as part of the Civilian Radioactive Waste Management Program. The YMP project is managed by the Waste Management Project Office of the U.S. Department of Energy, Nevada Operations Office. YMP Project work is sponsored by the DOE Office of Civilian Radioactive Waste Management.

URANIUM TRANSPORT IN TOPOPAH SPRING TUFF: AN ION-MICROSCOPE INVESTIGATION

K. D. McKeegan, D. Phinney, V. M. Oversby, M. Buchholtz-ten Brink, and D. K. Smith.
Lawrence Livermore National Laboratory, P.O. Box 808, Livermore, Calif. 94550.

ABSTRACT

We investigated the effect of different methods of surface preparation on ion-microscope profiles of uranium concentration (added to the sample by diffusion from an aqueous solution) vs depth in a welded, devitrified, tuffaceous rock from Yucca Mountain. The concentration profiles were used to study transport of uranium in the tuff. Four wafers of rock were prepared from primary drill core material and finished by polishing with increasingly finer abrasive material. Final polishes were made with 400 grit SiC, 600 grit SiC, 0.3 μ m alumina, and 0.05 μ m alumina. The polished tuff wafers were exposed for eight hours to a solution of groundwater doped with 2 ppm ²³⁵-U. The wafers were then examined by SEM and the ion microscope was used to measure the lateral and depth distributions of ²³⁵-U and other isotopes in the wafer. No systematic correlation of the measured ²³⁵-U concentration- vs-depth profiles with the degree of surface finish was observed, indicating that the polishing does not affect the measurable transport of U in the tuff. A zone of enhanced ²³⁵-U concentration was observed in the upper few microns, which we attribute to sorption onto surfaces of exposed pores. Concentrations of ²³⁵-U were elevated above background to depths > 15 μ m, indicating that rapid transport paths exist. When the uranium distribution near the surface of the wafer was modelled by an error function, an upper limit for a slower transport path was defined by an apparent diffusion coefficient of approximately 10^{-13} cm²/s.

INTRODUCTION

The rock used for this investigation is from the Topopah Spring tuff at Yucca Mountain, Nevada, the potential site of a high level waste repository. It is a welded, devitrified, rhyolitic tuff, which consists of a very fine-grained matrix of quartz, alkali feldspar, and cristobalite, with minor amounts of biotite, accessory phases, and a few phenocrysts [1]. The rock contains both macroscopic and microscopic fractures. We have previously studied the transport of uranium and plutonium through wafers of this tuff that had been included in glass waste form dissolution tests [2]. In this previous work we interpreted the measured concentration-vs-depth profiles using a simple model of diffusion between two homogenous media with a planar interface [3]. An error function was fit to each profile for depths from ~0.5 to ~5 μ m, yielding apparent diffusion

coefficients (D_{app}) in the range 10^{-17} to 10^{-16} cm²/s. The subscript "app" indicates that

these diffusion coefficients are apparent, having been calculated from a model that assumes a homogeneous medium and a single transport process by diffusion. Despite a relatively large spread in values calculated for different locations on a single wafer, there was some indication that the D_{app} was inversely correlated with exposure time. The

apparent time dependence was investigated in a second experiment wherein wafers of polished tuff were exposed (1 min to 14 days) to a solution of groundwater doped with 2 ppm ²³⁸-U [4]. Apparent diffusion coefficients from these experiments showed a linear array on a plot of log D_{app} vs log time.

McKeegan et al. [4] used an imaging detector called a resistive anode encoder (RAE) on the ion microscope, which allowed us to obtain the lateral distribution of uranium as an image at each depth during a depth profile. Imaging data were also obtained for silicon, lithium, aluminum, and zirconium. Depth profiling images allowed us to identify

regions of high background levels of naturally occurring ^{238}U (eg., zircon crystals) that complicated the diffusion analysis. To avoid difficulties identifying the tracer ^{238}U from the background ^{238}U , we have used ^{235}U as the tracer isotope in the work reported here.

The low values of D_{app} found in the earlier work [2] and the time dependence of the values, which suggested complex transport mechanisms, led us to investigate the effects of the method of preparation of the sample surfaces on the results. To do this, we prepared a series of tuff wafers with different degrees of surface finish and exposed the wafers to a solution containing ^{235}U for an eight hour period.

EXPERIMENTAL METHOD

Primary drill core material from hole USW H-6 (1109 feet below the surface) in the Topopah Spring tuff was cored with a 25 mm diameter, diamond-impregnated, stainless-steel core bit. The core was then sliced into wafers 2.2 mm thick using a low-concentration diamond wafering blade cooled with deionized water. Each wafer was cleaned in deionized water in an ultrasonic bath for 10 minutes or more, then air dried and weighed.

Four wafers were finished by polishing with increasingly finer abrasive material. Wafers were ground for about 5 minutes with medium hand pressure using 120 grit SiC mixed as a slurry with deionized water on a clean glass plate. After each grinding, samples were rinsed in deionized water and ultrasonically cleaned for 5 minutes. All wafers were then ground with 400 grit SiC, three with 600 grit SiC, two were polished with 0.3 μm alumina, and one was polished with 0.05 μm alumina and water on a low-nap polishing cloth.

All wafers were then ultrasonically cleaned, air dried, and scribed with fiducial marks, which were used to provide positive position markers for selection of analysis regions in the ion microscope.

The polished wafers were soaked for one week in J-13 water (a dilute sodium bicarbonate groundwater from a well located to the east of Yucca Mountain) to saturate the pore spaces. Each fluid-saturated wafer was then placed in a stainless steel holder that allowed access of fluid to all sides of the wafers. The holder and wafer were put into a polyethylene vial (previously conditioned with J-13 water) containing 15 ml of a solution of 2 ppm ^{235}U in J-13 water. This tracer solution was prepared by adding a few milliliters of ^{235}U in 0.8 N HCl to 100 mls of J-13 water buffered with NaHCO_3 . The resulting solution contained about 10 times as much sodium and bicarbonate as J-13 water. The wafers were left in the ^{235}U -doped solution for 8 hours at room temperature, then removed from solution, drained to remove surface water, and allowed to air dry.

Immediately after addition of the acid solution of ^{235}U , the tracer solution had a pH of 5.8. Additional NaHCO_3 was added and the pH rose to 7.8, measured just prior to the start of the experiment. The pH of the stock of tracer solution was measured several days after the conclusion of the wafer exposure and was found to be 8.8; a few weeks later, the pH had risen to 9.3. The equilibrium value for the solution, calculated from the concentrations of elements in solution and the partial pressure of CO_2 in the laboratory air, would be 9.5; the value expected for J-13 water would be 8.6. The observed variation in pH of the tracer solution is probably due to an initial over-pressure of carbon dioxide caused by the bicarbonate addition, followed by slow release of CO_2 gas from the solution through the walls of the plastic vials.

Prior to analysis, the wafers were vacuum dried at 64 $^{\circ}\text{C}$ and carbon coated for secondary (SEM) and backscattered (BSE) electron imaging. A portion of the 0.05 μm polished wafer was also coated with <200 nm of gold in a plasma-sputter coater (HUMMER VI)

at a pressure of $\sim 5 \times 10^{-2}$ Torr argon. Since the mean free path for the gold ions is about 1 mm under these conditions, the Au film effectively coats the surface of the tuff wafer without shadowing. This means that the interior walls of the exposed pores are also coated with gold. A JOEL 733 microprobe with typical operating conditions of 25kV and 10 to 15 nA beam current was used for examining the wafers. Photographs of the surface were taken at 40x, 100x, and 200x. A few representative areas were selected on the wafers finished with 400 and 600 grit SiC for ion microscope analysis. For the more highly polished samples, areas that showed a minimum of heterogeneity and surface topography in

the SEM and BSE images were selected for analysis, in order to simplify interpretation of the results.

Depth-profiling analyses were made with a CAMECA IMS 3F ion microscope. Positive secondary ions were measured for 8 masses (${}^7\text{Li}^+$, ${}^{11}\text{B}^+$, ${}^{28}\text{Si}^{++}$, ${}^{30}\text{Si}^+$, ${}^{27}\text{Al}^{++}$, ${}^{92}\text{Zr}^+$,

${}^{235}\text{U}^{16}\text{O}^+$, ${}^{238}\text{U}^{16}\text{O}^+$). Signals were either collected on the RAE, yielding sequences of lateral images versus depth (imaging depth profiles) or on the electron multiplier (EM) detector (conventional depth profiles). The ${}^{235}\text{U}$ tracer and ${}^{238}\text{U}$ were measured both on the EM and the RAE. Our measurement techniques conformed to the usual practice for depth-profiling with an ion-microscope [5]. For each area analyzed on the wafer surface,

a 100 μm X 100 μm crater was produced by sputtering with a rastered 17 keV ${}^{16}\text{O}^-$ primary beam. The primary beam current was typically 20 ± 5 nA and the beam diameter was about 25 μm . A field aperture in the secondary mass spectrometer was positioned such that sputtered ions were accepted only from the central 60 μm diameter portion of the rastered crater in order to better define the correlation of sputtered-ion intensity with depth. The sputtering process removes material from the sample surface, which was originally a planar area with irregularities caused by the intersection of pores with the surface.

For some profiles, the sputtering beam was reduced in current and high quality images of several major and minor elements were taken to facilitate comparison of ion-maps with

SEM and BSE images. The ${}^{235}\text{UO}^+$ ion intensity in the tuff was converted to a concentration by normalizing the ion yield to that determined for uranium in NBS glass SRM612. We estimate that the uranium concentrations are accurate to within a factor of two, and have a precision of approximately 10 % for values that are significantly above the background. The depths of the sputtered craters were measured with a Dektak IIA profilometer. Sputtering times were converted to depths by assuming a constant sputtering rate.

RESULTS

Imaging depth profiles were acquired for six different areas from both the 0.05 μm and 0.3 μm polished wafers, three areas were measured from the wafer finished to 600 grit, and two on the 400 grit wafer. Surface profilometer scans across a representative crater from each wafer are shown in Figure 1. The decrease in average surface roughness with increasingly finer polish is apparent, although it is important to note that significant topography, due primarily to pore spaces exposed to the surface, exists even for the highly polished wafers.

The measured ${}^{235}\text{U}$ concentrations are plotted as a function of depth for each crater in Figure 2. In all cases, the ${}^{235}\text{U}$ concentration is highest at the surface (i.e., within the first few tenths of a micron) and, with only two exceptions (both on the 0.3 μm polished wafer), decreases monotonically with depth. In no case does the ${}^{235}\text{U}$ decrease to its intrinsic background concentration of ~ 0.03 ppm (measured on an unexposed tuff wafer). This elevated background of the tracer ${}^{235}\text{U}$ persists to crater depths exceeding 15 μm in areas analyzed on both the most highly polished and the least polished wafers.

The ion images corresponding to the ${}^{235}\text{U}$ concentration-vs-depth profiles show that the tracer is heterogeneously distributed within the top few microns of each wafer. Nevertheless, when integrated over the imaged field of view of the ion microscope (~ 3000 μm^2 on the sample surface), the measured ${}^{235}\text{U}$ concentrations are the same for different craters (both on a given wafer and among different wafers) to within about a factor of five. This relative homogeneity is partly due to the fact that the areas analyzed were chosen to be representative of the fine-grained matrix of the tuff, avoiding known fractures and phenocrysts. (These criteria for selecting areas for depth profiling were not used in previous experiments [2]; therefore, the reader is cautioned against making direct comparisons of those depth profiles with the present work.) The homogeneity on this size scale also makes it possible to model the average transport of the dissolved ${}^{235}\text{U}$ tracer into the tuff based on the integrated concentration vs. depth data.

WAFER SURFACE PROFILES

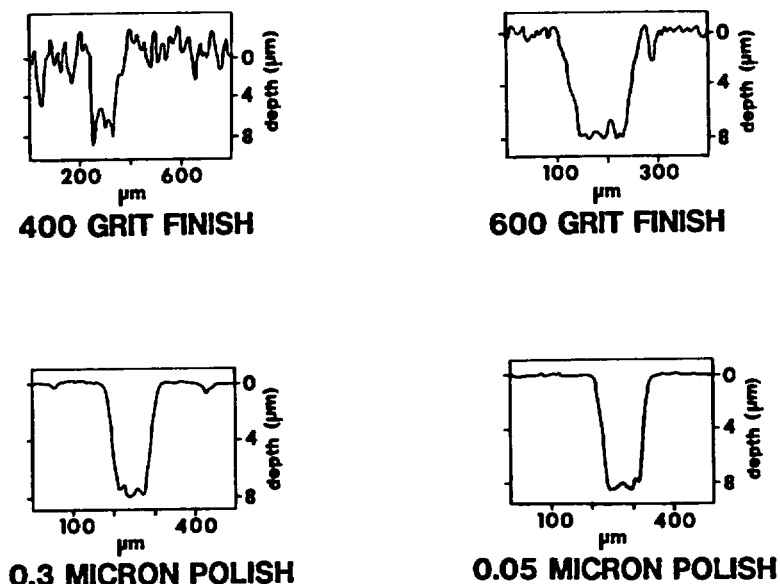


Figure 1. Dektak profilometer scans across representative craters from each of the four tuff wafers illustrating the topography for the different surface finishes.

The diffusion coefficients that result from a fit of an error function (e.g., Figure 3) to the ^{235}U concentration-vs-depth profiles range from 6×10^{-12} to $1 \times 10^{-13} \text{ cm}^2/\text{s}$ among the various spots analyzed on the four different wafers. In order to obtain the error function fits, it is necessary to subtract any elevated concentration of ^{235}U at depths greater than 5 to 10 μm as a "background" contribution arising from a volumetrically small fast transport component. In addition, because the surface roughness caused by exposed pores results in a larger tuff surface area being sampled by the ion beam at the surface than in the bulk tuff, the data from approximately the top micron cannot be used in the error function fit. The calculated apparent diffusion coefficients for each analyzed area and the depth range over which the concentration data were fit by the error function are summarized in Table 1.

DISCUSSION and CONCLUSIONS

The underlying assumptions used in interpreting the depth profiling data with an aqueous diffusion model are that the measured concentration of ^{235}U at a given sputtering time is proportional to the amount of ^{235}U transported during the exposure period through the tuff to a given depth and that transport occurs by a single diffusion mechanism. Of necessity the ion microscope measurements must be made in the region near a cut surface, as opposed to the interior of the tuff. The goal of the present experiment was to determine whether the method of surface preparation caused changes in the rock that affected uranium transport.

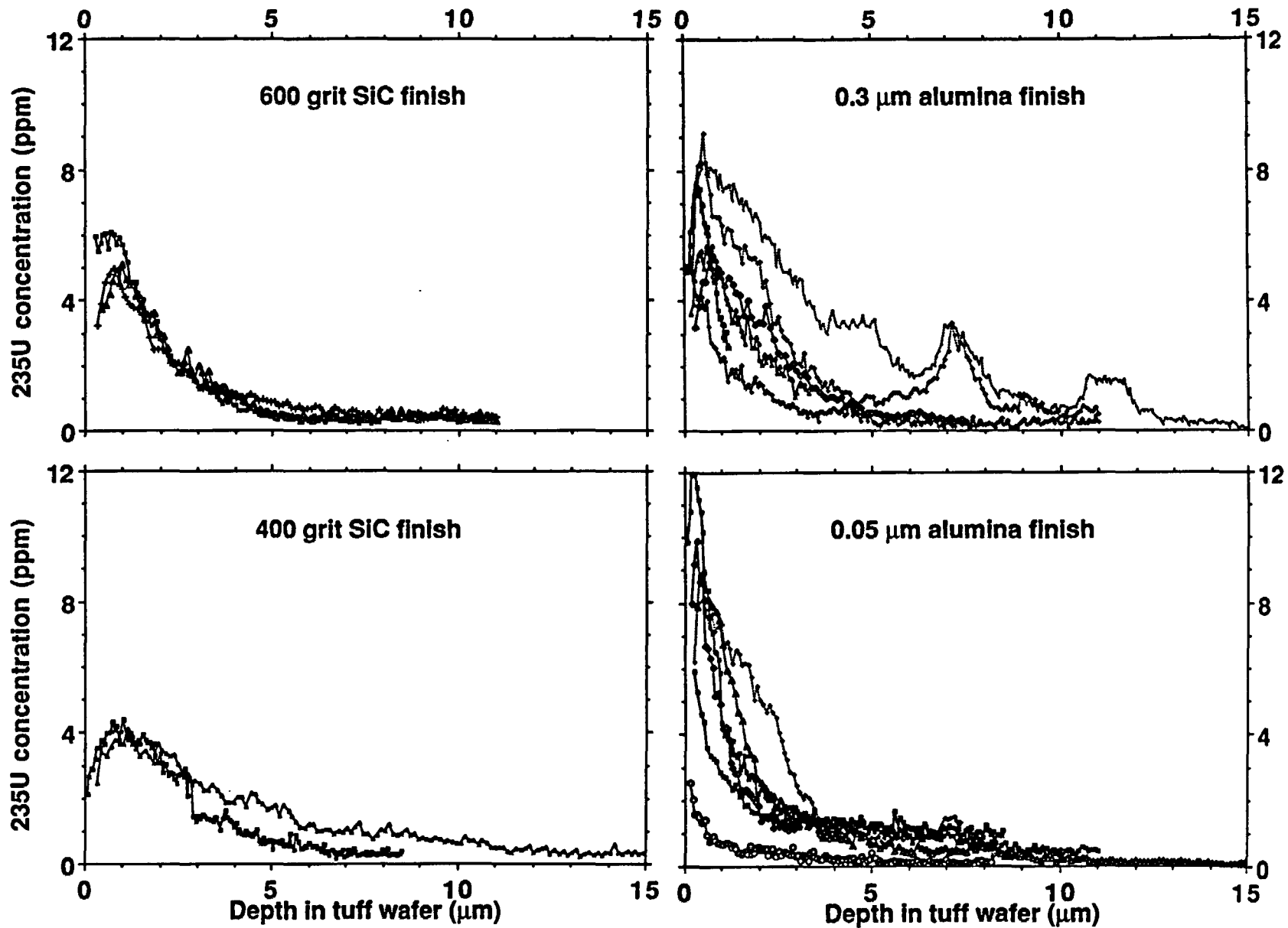


Figure 2. ^{235}U concentration vs. depth for each area analyzed on the tuff wafers with different surface finishes.

Table 1. Model parameters and calculated apparent diffusion coefficient values for ^{235}U in tuff.

Finish	Crater No.	Crater Depth (μm)	Range of fit depth (μm)	model C_0^* (ppm)	$C_{\text{bkgd}}^\#$ (ppm)	D_{app} ($10^{-13} \text{ cm}^2/\text{s}$)
0.05 μm	3	8.5	1.0 - 4.0	7.0	1.2	4.7
	4	17.0	0.8 - 8.0	9.3	0.2	10.1
	5	8.2	0.1 - 4.0	2.6	0.1	3.0
	6	4.2	0.3 - 2.4	12.3	1.2	1.4
	7	11.0	1.5 - 9.5	2.1	0.5	57.1
	8	10.5	0.3 - 7.5	9.7	0.4	9.0
0.3 μm	1	15.0	1.2 - 12.5	10.1	0.3	26.6
	2	1.3	0.4 - 1.3	11.5	0.6 ⁺	1.5
	3	3.3	0.7 - 2.9	7.9	1.3	3.7
	5	11.0	0.6 - 6.0	8.9	0.6	10.1
	6	7.5	0.8 - 5.2	6.7	0.4	11.5
	7	11.0	0.7 - 5.0	3.3	0.2	8.5
400 grit	1	8.0	0.9 - 6.0	5.8	0.4	13.5
	2	17.0	1.0 - 13.0	3.5	0.2	45.8
600 grit	1	7.8	1.2 - 6.0	8.1	0.4	7.3
	2	11.0	0.7 - 6.5	6.6	0.4	9.8
	3	11.0	0.9 - 7.8	5.5	0.5	11.5

*Model C_0 is the ^{235}U concentration required at the surface of the rock for the ^{235}U concentration within the "fit depth" to fit an inverse error function solution of the diffusion equation.

$C_{\text{background}}$ is the ^{235}U concentration deeper than the "fit depth" and, although it is greater than the natural ^{235}U concentration in the tuff, is assumed to be a background level for the purpose of fitting the data within the "fit depth" to an inverse error function solution of the diffusion equation.

+ Analysis was cut short due to analytical problems. Background value is the average of background values for other craters on the wafer with 0.3 μm finish.

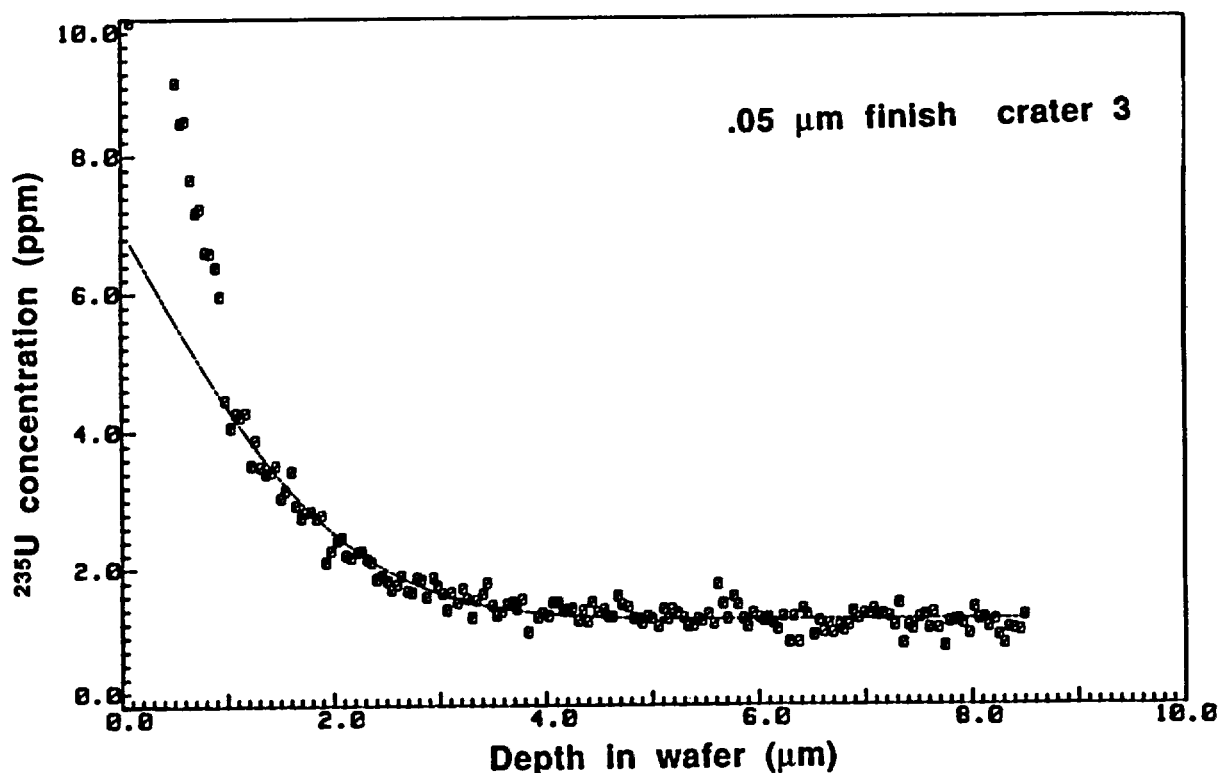


Figure 3. Error function fit to ^{235}U concentration-vs-depth profile for $D_{\text{app}} = 4.7 \times 10^{-13} \text{ cm}^2/\text{s}$.

From Figure 2 it is obvious that there are no systematic correlations of the measured 235-U concentration-vs-depth profiles with the degree of surface finish for the four different tuff wafers. The range of calculated diffusion coefficients (Table 1) for different areas on a given wafer overlaps those of the other wafers. We conclude, therefore, that the measured concentration profiles, and the limits on the transport of uranium into the tuff that these profiles define, are not artifacts produced by altering the physical properties of the tuff by polishing. The transport of the uranium into the rock is, therefore, assumed to occur by one or more of the following mechanisms: diffusion in the liquid phase in the pore structures, surface diffusion at the grain boundaries in the matrix material, sorption onto mineral phases, and evaporation from the residual liquid in the pores when the final samples are dried prior to analysis. We believe that the amount of material deposited by evaporation is small compared to that due to the other processes for regions of the sample near the wafer surface.

A second aspect of surface preparation that must be considered concerns the intrinsic geometry of the pore structures of the tuff. The cutting of any surface through the tuff exposes pores to the tracer solution that may not have been able to provide a transport path in the volume of the rock; i.e., some fraction of the exposed pores would have been "dead-end" pores in situ. The cutting also exposes the interiors of large pores, which may be connected to other pores by narrow channels. The effect of the re-entrant nature of the polished surface of the tuff is to broaden the concentration- vs-depth profiles for sorbing species, such as uranium. This effect has been demonstrated by depth profiling on the Au coated region of the 0.05 μm polished wafer. The Au depth profile in the tuff wafer is significantly broader than that in a polished, flat, non-porous Si wafer that was coated simultaneously with the tuff wafer (Figure 4). The RAE cross-section images (Figure 4) show that the Au film is able to coat at least some of the surface area available within the exposed pore space. In this same depth profile, the 235-U tracer also shows enhanced concentration in the same regions as the Au, although the 235-U does persist to deeper points in the tuff wafer. Because of the differences in exposure method, it is not possible to rule out that more exposed surface area was available to the 235-U in solution than to the Au in the plasma coater. Some of the 235-U signal at depth could be due to transport by a fast path, the existence of which is demonstrated by the elevated backgrounds of 235-U at depths much greater than the scale of surface topography (Table 1).

The Au profile on the 0.05 μm tuff wafer can be fit between ~ 1 and $2.5 \mu\text{m}$ by an error function with an apparent diffusion coefficient of $2 \times 10^{-13} \text{ cm}^2/\text{s}$ for a fictitious 8-hour exposure period. Therefore, we conclude that in this experiment it is not possible to distinguish rigorously between diffusional transport with apparent diffusion coefficients less than 10^{-12} to $10^{-13} \text{ cm}^2/\text{s}$ (the value depends on surface topography) and a static sorbed surface zone. The apparent diffusion coefficients reported in Table 1 must, therefore, strictly be considered as upper limits for the rate of transport of uranium by a mechanism with a time constant that is much less than that which characterizes the "fast" transport paths that produce the elevated 235-U signal at depths $> 10 \mu\text{m}$ in the rock. Based on depth profiling data in tuff wafers that had been exposed to 238-U and 239-Pu-doped J-13 water for 182 days [2], and on shorter exposures of wafers to 238-U [4], it is likely that the average effective diffusion coefficient for actinide transport

through the tuff matrix by the slow mechanism is less than $10^{-16} \text{ cm}^2/\text{s}$.

The present experiment did not expose the tuff wafers for sufficient time to produce a measurable effect that could be unambiguously attributed to transport of 235-U by slow-path diffusion through the tuff matrix. The lower intrinsic background of 235-U compared to 238-U has, however, enabled us to confirm the existence of several paths of aqueous transport through the rock with time constants that are similar to that expected for unimpeded ionic diffusion in an aqueous medium. In addition, the ion imaging capability has yielded new qualitative information concerning the nature of these fast transport paths. For example, ion images taken at $4.2 \mu\text{m}$ below the surface of the 0.05 μm polished wafer (Figure 5) show the 235-U concentrated in a crack or porous region on the boundary between what may have once been two glass shards (or possibly a phenocryst and a glass shard) that have since devitrified. The existence of this crack has been confirmed

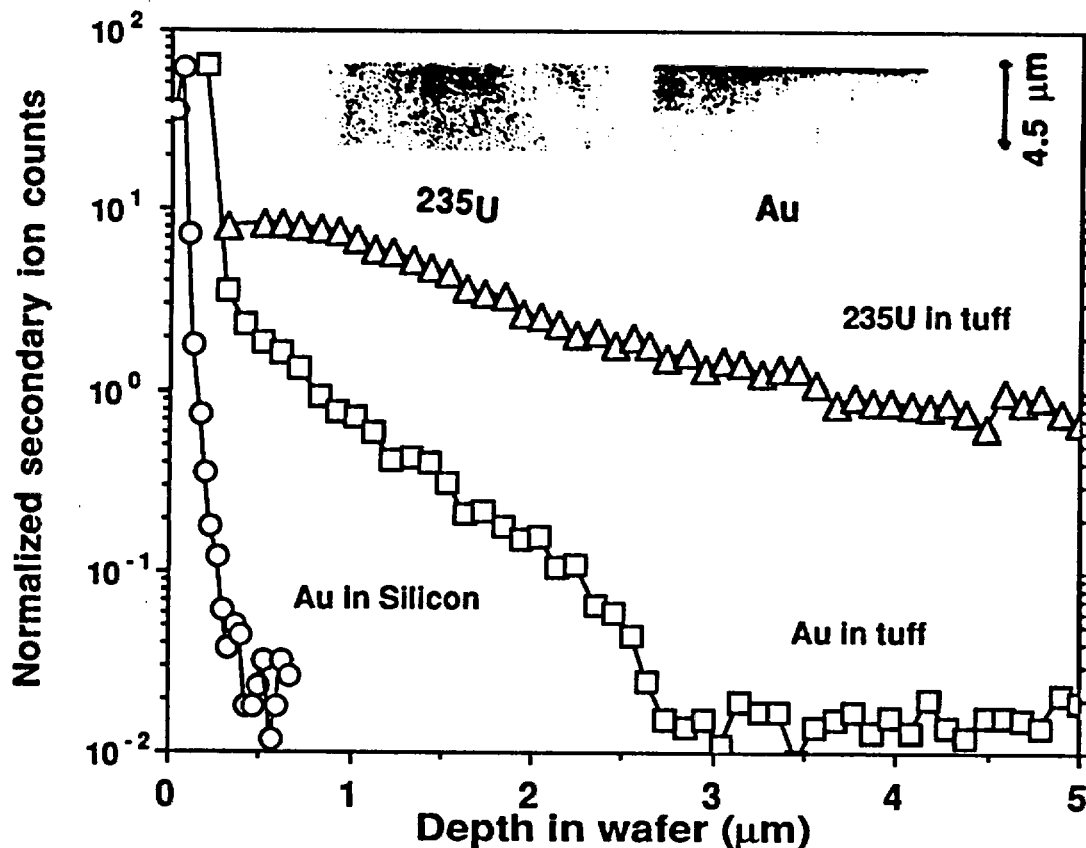


Figure 4. Depth profiles of a Au film on a silicon wafer and on the 0.05 μm polished tuff wafer. Also shown are the ^{235}U depth profile on the tuff wafer and cross-sectional images of the ^{235}U and Au distributions in depth in the tuff wafer.

by both surface profilometry and electron microscopy, even though it was not apparent on the SEM micrographs of the polished surface of the wafer prior to ion microscope analysis. Other examples show localized ^{235}U concentrations at depth that are not correlated with discernable petrographic features on the electron or ion images. It is apparent that it will take considerable effort to delineate the major and minor transport pathways for uranium in Topopah Spring tuff and to evaluate the relative importance of aqueous diffusion into dead-end pore space and through slow transport paths in the matrix of the rock.

REFERENCES.

- [1] F. M. Byers and L. M. Moore, Los Alamos National Laboratory Report No. LA-10901-MS, Los Alamos, New Mexico, 72 pp. (1987).
- [2] D. L. Phinney, F. J. Ryerson, V. M. Oversby, W. A. Lanford, R. D. Aines, and J. K. Bates. In: Materials Research Society Symposia Proceedings Vol 84, Scientific Basis for Nuclear Waste Management, Ed. J. K. Bates and W. B. Seefeldt. pp 433-446 (1987).
- [3] J. Crank, The Mathematics of Diffusion, Clarendon Press, Oxford, 414 pp. (1975).
- [4] K. D. McKeegan, M. R. Buchholtz-ten Brink, V. M. Oversby, and D. L. Phinney, EOS, 68(44), 1282 (1987).
- [5] E. Zinner, Scanning 3, 57-78 (1980).

This work was performed under the auspices of the U. S. Department of Energy by the Lawrence Livermore National Laboratory under contract No. W-7405-Eng-48.

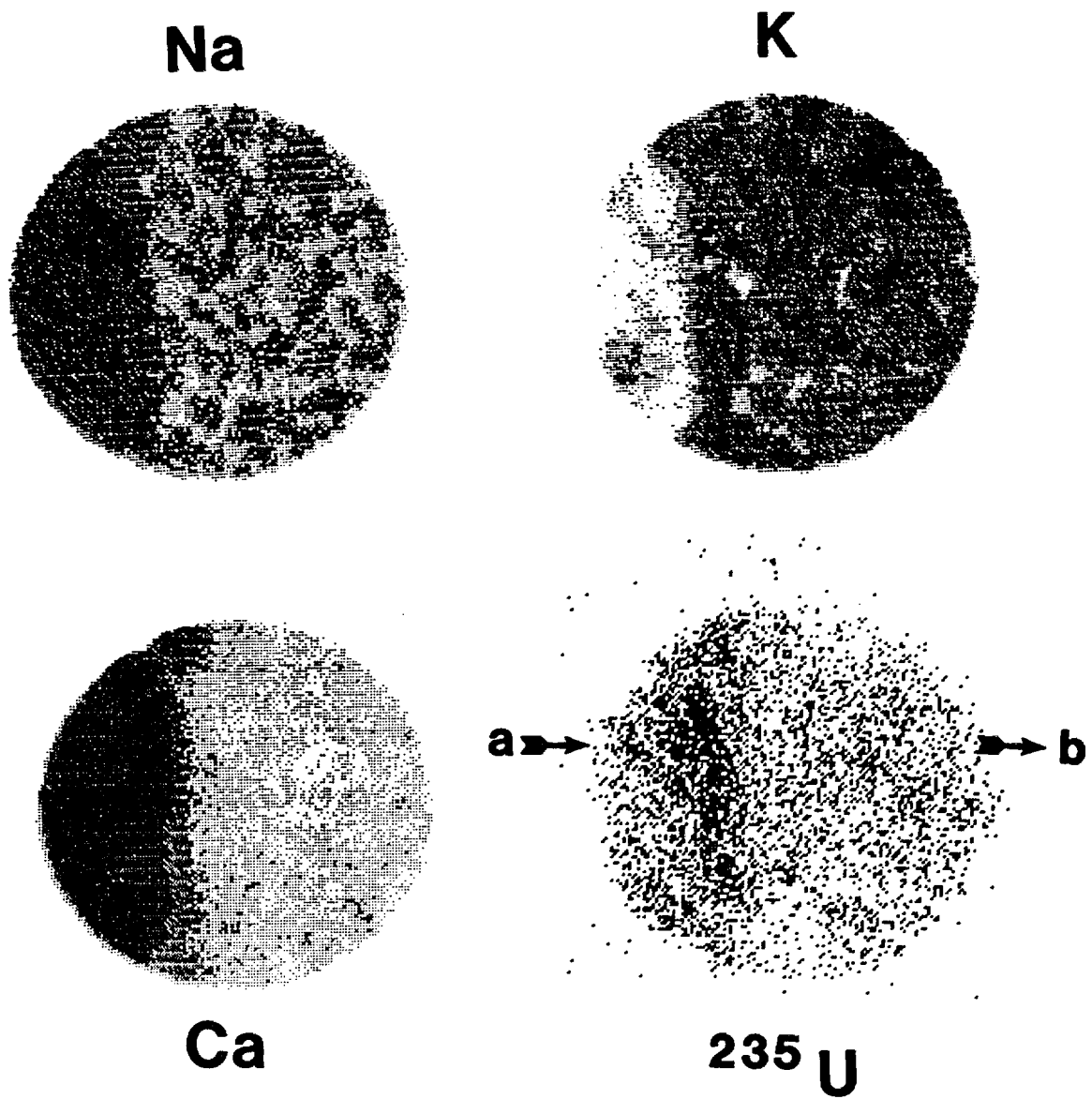
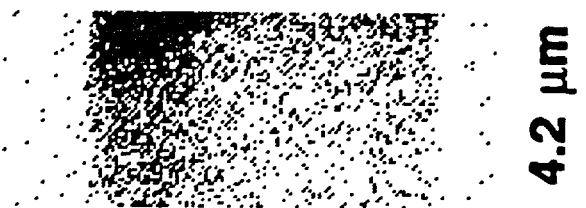


Figure 5. Ion images of the Na^+ , K^+ , Ca^+ , and $^{235}\text{UO}^+$ distributions in one $60\ \mu\text{m}$ diameter area of the $0.05\ \mu\text{m}$ polished wafer, and a cross-sectional image (lower right) taken along the line ab showing enhanced transport of ^{235}U to a depth of $4.2\ \mu\text{m}$.



4.2 μm

The following number is for Office of Civilian Radioactive
Waste Management Records Management purposes only and
should not be used when ordering this document:

Accession Number: NNA.881117.0006

Technical Information Department · Lawrence Livermore National Laboratory
University of California · Livermore, California 94550

